ACS Chemical Neuroscience

Research Article

pubs.acs.org/acschemicalneuroscience

Label-Free Detection of G Protein–SNARE Interactions and Screening for Small Molecule Modulators

Christopher A. Wells,[†,‡] Katherine M. Betke,[†,‡] Craig W. Lindsley,[‡,§] and Heidi E. Hamm*[,‡]

[‡]Department of Pharmacology and [§]Department of Chemistry, Vanderbilt University Medical Center, 442 Robinson Research Building, 23rd Avenue South @ Pierce, Nashville, Tennessee 37232-6600, United States

ABSTRACT: $G_{i/o}$-coupled presynaptic GPCRs are major targets in neuropsychiatric diseases. For example, presynaptic auto- or hetero-receptors include the D_2 dopamine receptor, H_3 histamine receptor, $5HT_1$ serotonin receptors, M_4 acetylcholine receptors, $GABA_B$ receptors, Class II and III metabotropic glutamate receptors, opioid receptors, as well as many other receptors. These GPCRs exert their influence by decreasing exocytosis of synaptic vesicles. One mechanism by which they act is through direct interaction of the G$\beta\gamma$ subunit with members of the SNARE complex downstream of voltage-dependent calcium channels, and specifically with the C-terminus of SNAP25 and the H3 domain of syntaxin1A. (Gerachshenko, T., Blackmer, T., Yoon, E. J., Bartleson, C., Hamm, H. E., and Alford, S. (2005) G$\beta\gamma$ acts at the C terminus of SNAP-25 to mediate presynaptic inhibition, *Nat. Neurosci. 8*, 597−605; Yoon, E. J., Gerachshenko, T., Spiegelberg, B. D., Alford, S., and Hamm, H. E. (2007) G$\beta\gamma$ interferes with Ca2+-dependent binding of synaptotagmin to the soluble N-ethylmaleimide-sensitive factor attachment protein receptor (SNARE) complex, *Mol. Pharmacol. 72*, 1210−1219; Blackmer, T., Larsen, E. C., Bartleson, C., Kowalchyk, J. A., Yoon, E. J., Preininger, A. M., Alford, S., Hamm, H. E., and Martin, T. F. (2005) G protein $\beta\gamma$ directly regulates SNARE protein fusion machinery for secretory granule exocytosis, *Nat. Neurosci. 8*, 421−425).[1−3] Small molecule inhibitors of the G$\beta\gamma$−SNARE interaction would allow the study of the relative importance of this mechanism in more detail. We have utilized novel, label-free technology to detect this protein−protein interaction and screen for several small molecule compounds that perturb the interaction, demonstrating the viability of this approach. Interestingly, the screen also produced enhancers of the G$\beta\gamma$−SNARE interaction.

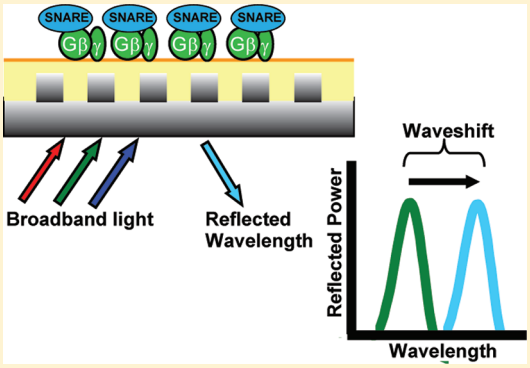

KEYWORDS: *Heterotrimeric G protein, protein−protein interactions, label-free detection, high-throughput screening, SNARE proteins*

Release of chemical transmitters by regulated exocytosis underlies many forms of intercellular communication. In the brain, neurotransmitter release is controlled by a series of intricate regulatory mechanisms, the best characterized of which includes formation of the SNARE (soluble *N*-ethylmaleimide-sensitive factor attachment protein receptors) complex. Formation of this complex occurs as the SNARE domains of three proteins: syntaxin, SNAP25, and synaptobrevin, interact to form a stable, four-helical bundle which brings the vesicle and presynaptic membranes into close proximity.[4,5] As intracellular calcium rises due to membrane depolarization, it induces a tight association between the SNARE proteins and the calcium sensor, synaptotagmin, bringing the vesicle into close apposition with the membrane.[6] In doing so, the energy barrier for fusion is reduced, and neurotransmitter is released into the synaptic cleft.[7] This simplistic view of fusion events is complicated by intricate interactions with a number of proteins that define stages in the process including priming, docking, and modes of fusion such as full fusion or kiss-and-run.[7] Such a complicated mechanism requires new techniques and probes to identify and define the importance of the spectrum of protein−protein and protein−lipid interactions that transpire.

G protein coupled receptors (GPCRs) are seven trans-membrane-spanning proteins that transduce extracellular signals such as hormones or light into intracellular pathways through heterotrimeric G proteins which consist of three subunits: Gα, which has a nucleotide-binding domain specifically for guanosine nucleotides, and G$\beta\gamma$, a functional dimer that dissociates from Gα upon activation of the heterotrimer by a stimulated GPCR. Activation is initiated via exchange of GDP for GTP in the Gα subunit, yet terminates through the actions of an inherent GTPase activity within Gα which hydrolyzes the terminal phosphate of GTP to result in a Gα-GDP with renewed affinity for binding to G$\beta\gamma$ and reforming the heterotrimer. $G_{i/o}$-coupled GPCRs play an intricate role in controlling neurotransmitter release as G protein $\beta\gamma$ subunits are known to interact directly with voltage-dependent calcium channels to inhibit calcium influx at the presynaptic terminal.[8−12] Examples of such GPCRs include adenosine, $GABA_B$, CB_1, and Group III mGlu receptors as

Received: October 18, 2011
Accepted: November 10, 2011
Published: November 10, 2011

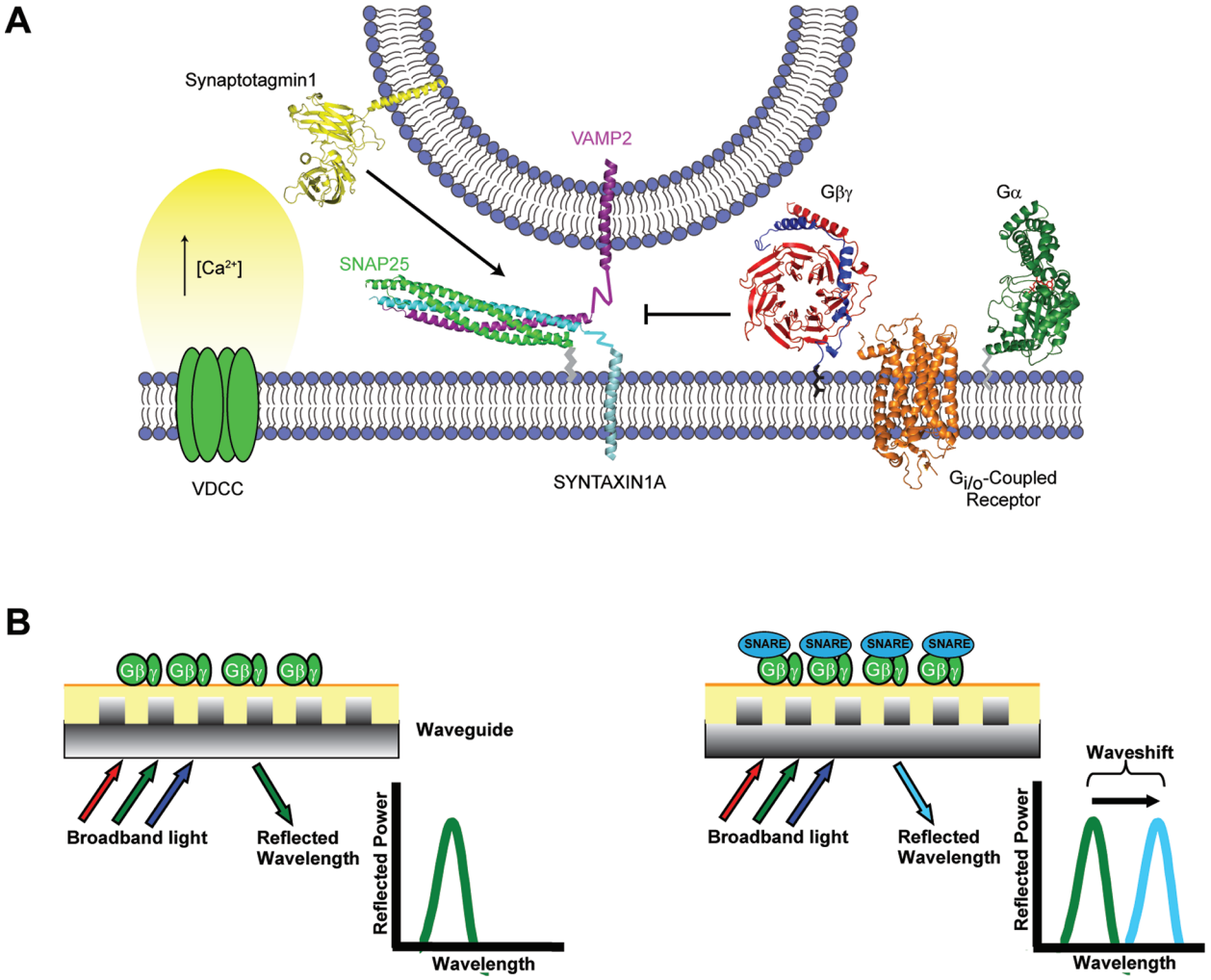

Figure 1. Role of G$\beta\gamma$ interaction with SNARE proteins and the scheme to detect that interaction with EPIC. (A) Upon activation of a presynaptic $G_{i/o}$-coupled receptor, G$\beta\gamma$ will interact with the ternary SNARE complex of VAMP2/SNAP25/Syntaxin1A. Upon sufficient elevation of intracellular calcium, synaptotagmin will be able to compete for interaction with the SNARE complex, displacing G$\beta\gamma$, and thereby promoting fusion of the synaptic vesicle. (B) G$\beta\gamma$ that is immobilized to the surface on the waveguide of the microplate will result in a specific reflected wavelength when exposed to broadband light. Binding of t-SNARE complex to immobilized G$\beta\gamma$ results in increased size and mass on the surface of the microplate, resulting in a reflected wavelength that will be shifted to a higher wavelength (waveshift, reported in picometers) when exposed again to broadband light.

demonstrated by Straiker et al. in their studies on cultured rat hippocampal cells.[13] In addition, $G_{i/o}$-coupled GPCRs are known to inhibit sites distal to calcium entry, with G protein $\beta\gamma$ subunits modulating synaptic transmission by binding directly to the SNARE proteins themselves, thereby limiting the number and duration of fusion events (Figure 1A).[2,3,14−16] We have shown that this direct effect on the exocytotic apparatus downstream of calcium entry works both on small clear synaptic vesicles as well as large dense core granules.[17] Additionally, such regulation of vesicle fusion by G$\beta\gamma$ has been reported by others in several areas of the brain,[18,19] as well as non-neuronal tissues such as the pancreas.[16] Further, this binding occurs in the same molecular region on the SNARE proteins as that seen for the calcium sensor, synaptotagmin, and a competitive interaction between G$\beta\gamma$ and synaptotagmin for binding SNARE has been demonstrated.[2] Thus, the effects of G$\beta\gamma$ on calcium channels and on the exocytotic fusion machinery may be additive or synergistic, and depend on synaptic activity.[2]

New methods are needed to study the novel association of G$\beta\gamma$ with SNARE and how it relates to SNARE binding with synaptotagmin or other binding partners in the regulated cascade of exocytosis. High-throughput screening systems would allow examination of binding partners, as well as permit testing of small molecule libraries which could later be taken forward into in vitro or in vivo assays of exocytosis. At present, the majority of screens require modification of one or more of the reaction components via enzymatic-, radio-, or fluorescent-labeling to report binding interactions. While such assays are robust in their responses, the addition of labels may interfere with molecular interactions by occluding binding sites or introduce significant background which limits signal-to-noise ratios.[20−22] Label-free technology is an emerging field that overcomes the need for labeling of one or more of the binding partners of interest.[20] Such technology is advantageous as it enables noninvasive and sensitive measurements of many cellular responses and protein−protein interactions, yet requires minimal manipulation of the reactants and does not suffer from potential assay artifacts seen in more traditional

dx.doi.org/10.1021/cn200102d | ACS Chem. Neurosci. 2012, 3, 69−78

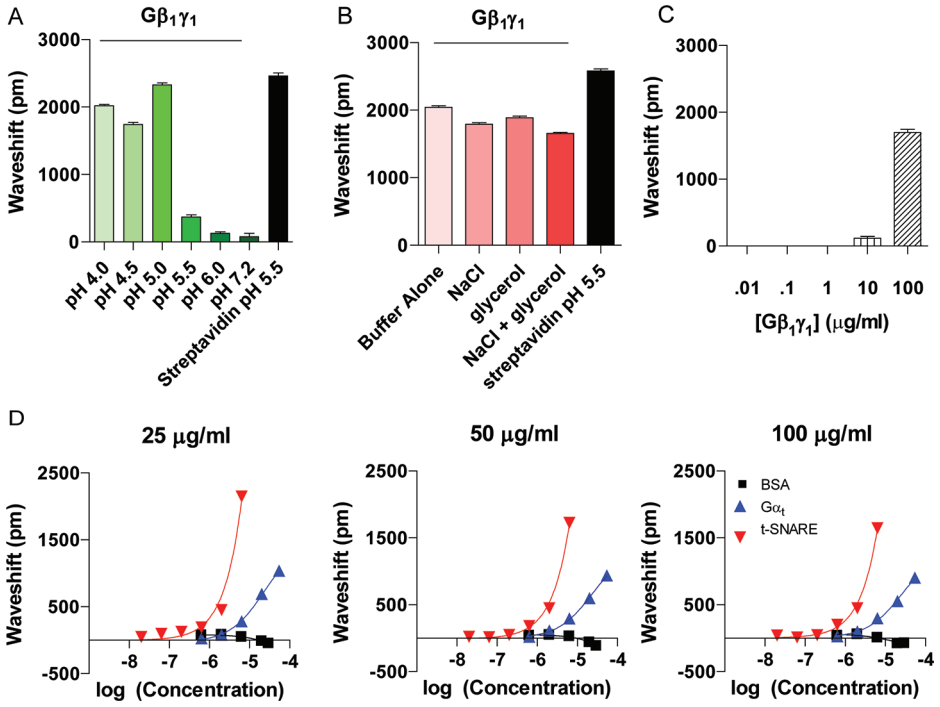

Figure 2. Optimization of immobilization of G$\beta\gamma$. (A) G$\beta_1\gamma_1$ was diluted in 20 mM sodium acetate of varying pH from 4.0 to 7.2 to a final concentration of 25 μg/mL. Streptavidin was mixed in 20 mM sodium acetate, pH 5.5 as a control. After allowing to immobilize overnight and quenching the remaining aminereactive coupling on the plate, plates were washed, thermally equilibrated within the EPIC plate-reader, and then an immobilization read was measured. Shown are the averages and SEM over 64 wells for pH 4.0–6.0, and 16 wells for pH 7.2 and for streptavidin. (B) G$\beta_1\gamma_1$ was diluted into 20 mM sodium acetate, pH 5.0 either alone, with 100 mM sodium chloride, 5% glycerol, or a combination of both. Again, streptavidin was added as control as in (A). After overnight immobilization, washes, and thermal equilibration, an immobilization measurement was taken. Shown are the averages and SEM over 64 wells for buffer alone, NaCl, and glycerol; 128 wells for NaCl + glycerol; and 16 wells for streptavidin. (C) G$\beta_1\gamma_1$ was diluted to varying concentrations as shown in 20 mM sodium acetate, pH 5.5. As above, the plate was washed and thermally equilibrated prior to an immobilization read being taken. Shown are the averages and SEM over 48 wells. (D) G$\beta_1\gamma_1$ was immobilized on plates at three concentrations that were detectable during immobilization reads, 25, 50, and 100 μg/mL. Immobilization reads were taken the next day as above. After the initial read, increasing amounts of t-SNARE, Gα_t, or BSA were exposed to the plate for one hour. A second read was performed with resulting waveshifts in the presence of those additional proteins shown. t-SNARE complex (red triangles) and Gα_t (blue triangles) resulted in an increase in waveshift, whereas BSA (black squares), a protein not expected to bind to G$\beta_1\gamma_1$, had no increase in waveshift at all concentrations tested. Binding curves were similar across the three immobilization concentrations performed. Shown are the averages and SEM over five wells for each point on each of the curves.

methods, such as autofluorescence.[21,23] Innovations in this field include impedance-based, optical biosensor-based, automated patch clamp, and mass spectrometry technologies, to name a few; however, for the sake of this Article we will focus solely on optical biosensors (for detailed review of these and other label-free technologies, please see refs 20–23).

Optical biosensor-based technologies include surface plasmon resonance and resonant waveguide grating (RWG), both of which use evanescent waves to characterize changes in refractive index at the surface of a sensor. In the case of surface plasmon resonance, light energy is transferred to electrons on a metallic surface, resulting in the propagation of charged density waves, surface plasmons, along the surface of the metal.[20,21] When the surface of the metal is exposed to polarized light, a reduction in the amount of reflected light is observed due to the resonant transfer of energy from the incoming light to the surface plasmons generated at the metal interface.[20,21] As a result, by monitoring the shift in the observed resonant angle, it is possible to detect molecular binding events in real time. Similarly, RWG also employs an evanescent wave for detection. In this case, however, RWG uses a nanograting structure to couple light into a waveguide composed of plastic and a thin dielectic coating via diffraction, in order to generate the wave.[21,23] By then exposing the sensors to wide spectrum light and measuring changes in the wavelength of the light that is reflected, it is possible to analyze biomolecular interactions.

Such technology was recently developed by Corning to detect protein–protein interactions. Immobilization of a target protein to a 384-well plate can be screened for its ability to interact with various binding partners by measuring waveshifts at the surface of the plate, with changes proportional to changes in mass and indicative of binding interactions. When incorporated with liquid handling, this technology permits high-throughput screening both of potential binding partners, as well as small molecules that may inhibit or enhance that interaction.

■ RESULTS AND DISCUSSION

The ability of G$\beta\gamma$ to directly bind to SNARE proteins has been previously determined.[2,3,14–16] Small molecules that can alter this interaction are needed to evaluate and manipulate it at a cellular level to further investigate exocytosis and the role that G$\beta\gamma$ plays in its regulation. High-throughput screening of this bimolecular interaction would be advantageous not only for characterizing the protein–protein interactions but also for development of small molecule modulators that would allow further definition of the role of this interaction in cells and

dx.doi.org/10.1021/cn200102d | ACS Chem. Neurosci. 2012, 3, 69–78

tissues. In this study, we sought to develop a method to examine Gβγ/SNARE interactions in vitro using this label-free technology. After establishing conditions necessary to reproducibly immobilize Gβγ and bind SNARE proteins, a library of biased protein−protein modulator ligands was screened to examine the ability of individual compounds to alter this interaction. This library has compounds containing a piperidine benzimidazolone moiety, a well-known GPCR privileged structure that has been shown to enhance protein−protein interactions between the pleckstrin homology (PH) domains and the catalytic domains of both Akt, a kinase, and phospholipase D, a lipid signaling enzyme.[24−29] Use of the Corning EPIC in this manner resulted in the discovery of three compounds with 50−100 μM activity that represent lead compounds in iterative development of small molecular probes that affect the ability of Gβγ to bind to SNARE proteins.

Protein Immobilization. Binding interactions between Gβγ subunits and SNARE proteins were evaluated using the EPIC system. The experimental scheme began with covalently immobilizing purified $G\beta_1\gamma_1$ or $G\beta_1\gamma_2$ to the surface of a microplate as depicted in Figure 1B through primary amine coupling chemistry in a 384-well microplate. Changes in waveshift were used to evaluate the effects of compound addition on t-SNARE binding to Gβγ.

To optimize immobilization of the Gβγ dimer to the plate, we tested the pH, salt, and glycerol-dependence. The pH dependence of $G\beta_1\gamma_1$ attachment to the plate was investigated by varying pH from 4.0 to 7.2. As can be seen in Figure 2A, the largest waveshift detected occurred at a pH of 5.0. This waveshift was comparable to that obtained for a positive control, streptavidin. Selecting the optimal sodium acetate buffer of pH 5.0, the buffer was then further tested for the effect of other reagents on the ability to immobilize Gβγ to the plate. The addition of 100 mM sodium chloride, 5% glycerol, or a combination of both, to the 20 mM sodium acetate immobilization buffer yielded no changes in waveshift as seen in Figure 2B. To test for saturation of immobilization of Gβγ, serial dilutions of Gβγ were exposed to a microplate overnight and analyzed the next day. As can be seen in Figure 2C, there was a steep decline in immobilized protein as detected by the EPIC plate-reader below a Gβγ concentration of 10 μg/mL. Based on the above data, the optimal immobilization buffer used for all subsequent assays was 20 mM sodium acetate, pH 5.0, and 5% glycerol.

We then turned to optimization of binding of partner proteins to Gβγ to establish conditions which would allow optimal detection of interaction with SNARE proteins. We altered the concentration of Gβγ immobilized over the range of 25−100 μg/mL. The partner protein of Gβγ, $G\alpha_t$, was successfully detected at all Gβγ protein immobilization concentrations, although not to saturation. Similarly, we could detect the binding of t-SNARE to the plate. Over this range of concentrations of immobilized Gβγ, there was no effect on the ability of t-SNARE to bind as seen by similar waveshifts in all cases (Figure 2D). We also included a negative control, bovine serum albumin (BSA), a protein with no expected binding affinity for Gβγ. It had no measurable interaction with Gβγ bound to the microplate.

Optimization of Ligand Interaction. After optimizing Gβγ immobilization, the binding of t-SNARE was then optimized. As noted above, immobilization of differing amounts of Gβγ had little or no effect on t-SNARE binding as measured by the waveshift. However, selection of a buffer to perform the binding did have an effect. Initially, the presence or absence of sodium chloride or glycerol was tested compared to buffer alone, 20 mM HEPES, pH 7.5. The presence of 100 mM sodium chloride appeared to attenuate the signal of t-SNARE binding to Gβγ as seen in Figure 3A. Conversely, the addition

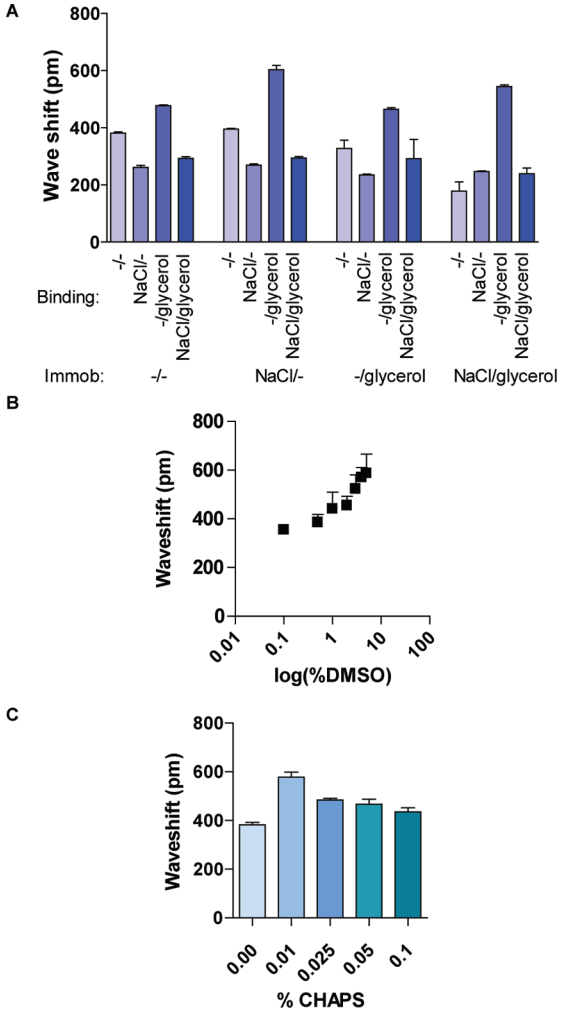

Figure 3. Optimization of the detection of t-SNARE binding to immobilized $G\beta_1\gamma_1$. (A) $G\beta_1\gamma_1$ was immobilized to the microplate in 20 μM sodium acetate, pH 5.0 either alone, or in the presence of 100 mM NaCl, 5% glycerol, or both. After washing, t-SNARE was then diluted to 2uM in either binding buffer alone, or with addition of 100 mM NaCl, 5% glycerol, or both. Shown are the averages and SEM over four wells. (B) Varying amounts of DMSO ranging from 0.1 to 5% was added to the binding buffer when a fixed concentration of t-SNARE was exposed to immobilized $G\beta_1\gamma_1$. The waveshifts detected are similar to that without any addition of DMSO. Shown are the averages and SEM over five wells. (C) Varying amounts of a detergent, CHAPS, from 0.01 to 0.1% were added to the binding buffer to assess effect of presence of detergent on detection of t-SNARE binding to $G\beta_1\gamma_1$. The waveshifts detected in the presence of CHAPS are similar to that obtained without the presence of the detergent. Shown are the averages and SEM over five wells.

of glycerol to the binding buffer improved the signal detected as compared to buffer alone. In fact, across almost all immobilization and binding conditions, a binding buffer of 20 mM HEPES, pH 7.5 that included 5% glycerol yielded significantly higher waveshifts ($p < 0.001 - p < 0.05$). Based on this result, binding buffers contained 5% glycerol.

dx.doi.org/10.1021/cn200102d | ACS Chem. Neurosci. 2012, 3, 69−78

Two other binding buffer variables explored included the effect on waveshifts in the presence of DMSO or detergent. DMSO concentrations were examined as the small molecules to be screened were dissolved in 100% DMSO. The EPIC system was reported to be able to tolerate up to 5% DMSO without an effect on the signal or deterioration of the plate. A wide variety of DMSO concentrations were examined for their effect on the waveshift detected during the interaction between t-SNARE protein and immobilized G$\beta\gamma$. As seen in Figure 3B, no degradation of signal was apparent in the presence of DMSO up to 5%, the maximum concentration allowable for screening. Similarly, to evaluate if a detergent affected the detection of t-SNARE−G$\beta\gamma$ interactions, the effect of addition of various concentrations of CHAPS was tested. Figure 3C shows that the addition of up to 0.1% CHAPS did not deteriorate the signal detected when t-SNARE was exposed to immobilized G$\beta\gamma$, although it did statistically increase the waveshift detected in the presence of t-SNARE. CHAPS was not included in the final buffer to simplify the constituents of that buffer. Additionally, 10 μM GDP and 2 mM magnesium chloride were added to all buffers as they are necessary for stability of the Gα subunit. In each case, no deleterious effect on signal was observed.

As seen in Figure 4A, Gα_t and t-SNARE had significantly increased waveshifts when compared to G$\beta\gamma$ exposed to buffer alone or BSA. To examine whether the binding between G$\beta\gamma$ and Gα was physiologically relevant, we tested the ability of Gα-GTPγS to bind to G$\beta\gamma$. This nonhydrolyzable guanine nucleotide decreases the affinity of Gα for G$\beta\gamma$ subunits, and as such would be expected to reduce binding of Gα to immobilized G$\beta\gamma$. As expected, the addition of GTPγS reduced the detected waveshift of Gα_t significantly ($p < 0.0001$) compared to GDP- Gα_t. Concentration response curves were generated examining the ability of increasing concentrations of t-SNARE, Gα_t, or BSA to bind to immobilized G$\beta\gamma$. As was seen with t-SNARE, waveshifts detected for Gα_t increased in a concentration dependent manner, Figure 2D. Similarly, the ability of immobilized G$\beta\gamma$ to recognize and interact with another binding partner, Gα_i was also explored, Figure 4B. As seen for Gα_t, Gα_i was also able to bind to immobilized G$\beta_1\gamma_1$ in a concentration dependent manner. Again, similar concentrations of BSA demonstrated very little change in waveshift when compared with those found with t-SNARE or Gα_i. When compared to Gα_t, Gα_i produced a greater waveshift when exposed to the same concentration of t-SNARE. However, when compared to t-SNARE, Gα_i had very similar waveshifts across multiple concentrations, Figure 4B. The difference between Gα_i and Gα_t is either due to plate-to-plate differences, or the specific activity of our source of Gα_t was reduced compared to Gα_i and therefore bound less.

Finally, the interaction of t-SNARE with another G$\beta\gamma$ dimer, G$\beta_1\gamma_2$, was determined to explore both if a different dimer could be immobilized and participate in binding as has been demonstrated with G$\beta_1\gamma_1$, as well as to determine if differences in waveshift would be detected depending on the G$\beta\gamma$ isoform immobilized. Immobilization of G$\beta_1\gamma_2$ was comparable to that of G$\beta_1\gamma_1$, Figure 5A. Concentration response experiments were carried out with results shown in Figure 5B. G$\beta_1\gamma_1$ and G$\beta_1\gamma_2$ both had similar concentration response curves as seen with the increase in waveshift with increasing concentrations of t-SNARE bound to the respective G$\beta\gamma$ dimer.

Use of EPIC in High-Throughput Screening of a Chemical Library. As the detection method for protein−protein interactions seemed reproducible and robust, we chose to use it in a search for small molecule modulators of the G$\beta\gamma$−SNARE interaction. The initial library was designed based on known chemotypes which modulate protein−protein interactions (α-helical mimetics, β-turn mimetics (types I−VI), flat surface interaction ligands)[30,31] as well as GPCR-biased ligands known to enhance protein−protein interactions[24−29] with compounds added simultaneously with t-SNARE to react with the immobilized G$\beta_1\gamma_1$. Compounds were added at a final concentration of 250 μM using a volume equal to that in the well, with stock concentrations of 500 μM in DMSO. Final well volume was 40 μL in each well. Waveshifts were assessed in at least four replicates for each compound in the presence or absence of t-SNARE.

Screening of this library of biased protein−protein modulator ligands[24−29] identified four lead compounds from two structural series (Figure 6A), three of which greatly diminished the waveshift produced upon G$\beta\gamma$ binding to SNARE (63V,

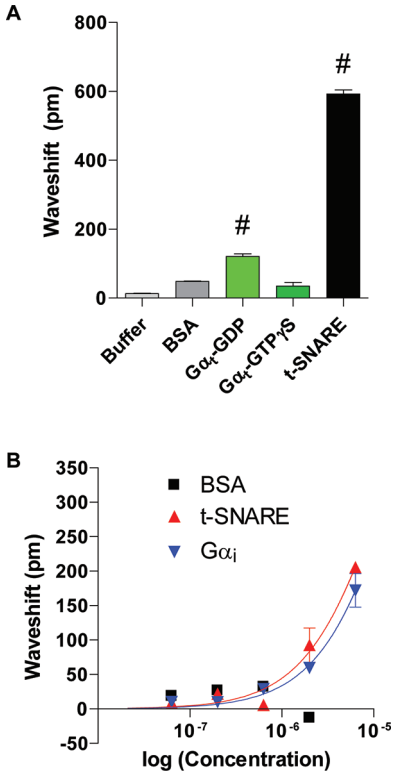

Figure 4. Evaluation of binding of immobilized G$\beta\gamma$ by Gα_t and Gα_i. (A) G$\beta_1\gamma_1$ was immobilized as described previously. Equal concentrations of Gα_t-GDP, Gα_t-GTPγS, BSA, and t-SNARE were allowed to bind to the immobilized G$\beta\gamma$ for 1 h before a read was taken. The waveshift for Gα_t-GDP was significantly different from buffer alone, BSA, or Gα_t-GTPγS, suggesting that Gα_t-GDP was binding to immobilized to G$\beta\gamma$. The t-SNARE had a significantly greater waveshift than Gα_t-GDP, as well as the waveshifts for buffer, BSA, and Gαt-GTPγS. Shown are averages with SEM for at least 12 wells on the plate. (B) G$\beta_1\gamma_1$ was immobilized as described previously. Increasing amounds of t-SNARE, Gαi, and BSA were exposed to the plate for 1 h. A second read was performed with resulting waveshifts in the presence of those additional proteins shown. t-SNARE complex (red triangles) and Gαi (blue triangles) resulted in an increase in waveshift whereas BSA (black squares), a protein not expected to bind to G$\beta_1\gamma_1$, had no increase in waveshift at all concentrations tested. Shown are averages and SEM over five wells on the plate for each point on the concentration response curves.

dx.doi.org/10.1021/cn200102d | ACS Chem. Neurosci. 2012, 3, 69−78

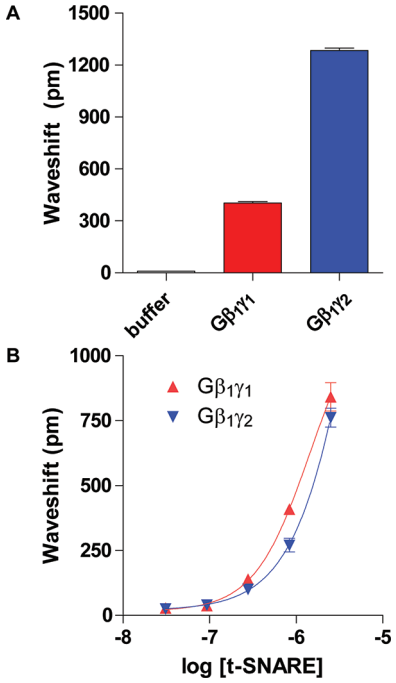

Figure 5. Similarity between immobilized G$\beta\gamma$ dimers binding to t-SNARE. (A) G$\beta_1\gamma_2$ (blue) was immobilized onto the microplate in previously described buffer alongside G$\beta_1\gamma_1$ (red). G$\beta_1\gamma_2$ appeared to have an increased immobilization efficiency with the plate as seen by the greater increase in initial waveshift detected after the immobilization step. Data shown are averages with SEM over 126 wells for G$\beta_1\gamma_1$, 126 wells for G$\beta_1\gamma_2$, and 16 wells for buffer alone. (B) This difference did not result in a difference in binding of t-SNARE. Increasing amounts of t-SNARE were exposed to the immobilized G$\beta\gamma$ dimers with a corresponding increase in waveshift. There was very little difference between fitted curves for binding to the two isoforms. Each point on the curves are the averages with SEM over at least four wells on the plate.

85M and 85B) and one (6EQ) which significantly enhanced it. An example of a screen of thirty of the initial 69 compounds is shown in Figure 6B. Nonspecific binding (as measured by SNARE binding to streptavidin coated wells) was subtracted from the G$\beta\gamma$-SNARE binding signal, resulting in the black line for the basal level of binding. By comparison to the waveshift achieved by interaction with t-SNARE alone (yellow column), most compounds had minimal to no effect. Based on the activities of the first four hits, further iterative synthesis and screening of related small molecules resulted in the discovery of additional compounds with modulatory effects on the interaction of G$\beta\gamma$ with t-SNARE.

To further examine lead compounds mentioned above as well as a number of other compounds in the initial screen, concentration response curves were obtained for those that showed a possible effect on the interaction of G$\beta\gamma$ with t-SNARE. The respective compounds were tested over the given range with at least replicates across 4 wells. These studies demonstrate that a signal of sufficient intensity using low volumes in a 384 well plate can be easily detected. The structures for representative lead compounds are shown in shown in Figure 7A with concentration response curves for each of those compounds in Figure 7B. Compound 85M (see screen in Figure 6A) appeared to be a weak inhibitor at higher (μM) concentrations with an estimated EC_{50} of 100 μM, Figure 7B. Compound 634 and 8HA were selected based on an initial screen of the remaining 39 compounds from the library (data not shown). Compound 634 appeared to be a weak enhancer of the interaction of t-SNARE with immobilized G$\beta\gamma$ with an estimated EC_{50} of 10 μM. Lastly, compound 8HA also appeared to be a weak enhancer with an estimated EC_{50} also of 10 μM. Current efforts are directed to making derivatives of these lead compounds with improved potency.

SIGNIFICANCE

The label-free EPIC system provides a novel means to screen for modulators of protein−protein interactions in an in vitro setting with scalability to high-throughput screening of libraries of compounds. The ability of t-SNARE to bind immobilized G$\beta\gamma$ in this assay is reproducible and physiologically relevant as shown by the ability to correctly assess G$\beta\gamma$'s interaction with its cognate partner Gα in the presence of GDP but not in the presence of GTPγS. This system allows relevant testing of an interaction between two unlabeled proteins. As well, the immobilized G$\beta\gamma$ dimer was able to interact with other known ligands, $G\alpha_t$ and $G\alpha_i$. Although immobilized G$\beta\gamma$ had a higher affinity for t-SNARE than its cognate partner Gα, we expect this difference is due to this system being a plate-based assay. In solution, we would expect Gα to have a higher affinity for G$\beta\gamma$. The ability for either Gα or t-SNARE to bind G$\beta\gamma$ suggests not only the physiologic relevance of the detected interaction, but also further generalization of the EPIC for extending this initial work to examining other interactions with immobilized G$\beta\gamma$ dimers in the future, such as other Gα subunits or other effectors such as phospholipase B, phosphoinositide 3-kinase, or interaction of other G$\beta\gamma$ isoforms with other Gα subunits or effectors. Furthermore, initial screens have yielded compounds that either weakly inhibit or enhance the interaction of G$\beta\gamma$ with t-SNARE. The compounds are the subject of further refinement for potency, efficacy, and selectivity. As well, this system is readily adapted to structure−function studies of mutant G$\beta\gamma$ or SNARE proteins or screening of peptides from the interaction surface for their ability to modulate the interaction of G$\beta\gamma$ with t-SNARE (data not shown).

The direct interaction of G$\beta\gamma$ with the exocytotic machinery to regulate exocytosis has been shown in multiple areas of the brain[2,15,18,32] as well as in chromaffin cells[33] and β cells of the endocrine pancreas.[16] There is a need to understand the physiological relevance of this interaction in further detail. Compounds specific for this interaction that either inhibit or potentiate the interaction would allow imaging and electrophysiological studies of synaptic exocytosis. The generality of this inhibitory mechanism on exocytosis, working both on small clear vesicles at synapses as well as large dense core vesicles, leads to the possibility that the effects of these small molecule inhibitors and enhancers of the G$\beta\gamma$-SNARE interaction may affect the workings of many synapses. By their drug-like nature, the small molecule compounds that have emerged from this screen would likely pass through the cell membrane, and thus following testing of their specificity for the G$\beta\gamma$ − t-SNARE interaction, could be used in cellular and tissue settings such as slice preparations. Such studies have the potential to greatly enhance our understanding of the role of G$\beta\gamma$ regulation of exocytosis in vitro. Future studies will optimize these initial tool compounds into potent druglike modulators with properties suitable for evaluation in vivo, including enhanced bioavailability and central penetration.

dx.doi.org/10.1021/cn200102d | ACS Chem. Neurosci. 2012, 3, 69−78

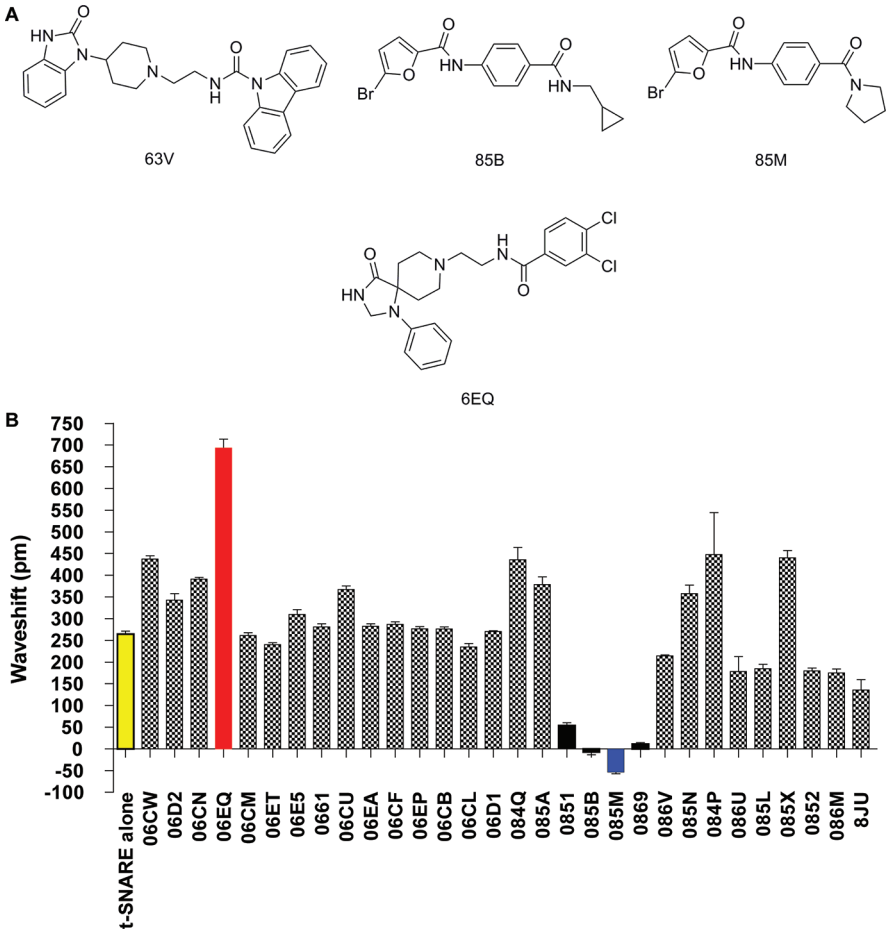

Figure 6. Screening of chemical compounds for modulation of $G\beta_1\gamma_1$ binding to t-SNARE. (A) Shown are the chemical structures for four compounds from an initial screen of a library of compounds that had a waveshift detected that differed significantly from the waveshift for t-SNARE alone exposed to immobilized $G\beta_1\gamma_1$. (B) $G\beta_1\gamma_1$ was immobilized overnight as described before. For each compound listed in the bar graph, a compound was mixed either with buffer alone in four wells, or buffer with 2 μM t-SNARE in four wells, and allowed to thermally equilibrate before a binding read was taken. The waveshift of buffer alone with compound was subtracted from that of compound with t-SNARE, with the difference shown in the bar graph. For comparison, t-SNARE alone without compound in eight wells of this plate was seen to have an average waveshift of 265 pm shown in the first column (yellow). Red signifies an example of a compound that enhanced the waveshift, black signifies compounds that significantly reduced the waveshift, and blue is a compound that significantly reduced the waveshift and showed a concentration dependent reduction in waveshift (Figure 7). Error bars shown are SEM.

METHODS

Plasmids. The open reading frames for the SNARE component proteins were subcloned into the glutathione-s-transferase (GST) fusion vector, pGEX6p1, (GE Healthcare, Chalfont St. Giles, Buckinghamshire, U.K.) for expression in bacteria.

Preparation and Purification of SNARE Proteins. Recombinant bacterially expressed GST fusion proteins were expressed in *Escherichia coli* strain BL21(DE3). Protein expression was induced with 0.1 mM isopropyl β-D-thiogalactoside for 16 h at room temperature. Bacterial cultures were pelleted, washed with 1× phosphate-buffered saline, and then resuspended in lysis buffer [50 mM NaCl, 50 mM Tris, pH 8.0, 5 mM EDTA, 0.1% Triton X-100, 2 mM phenylmethylsulfonyl fluoride, and 1 mM dithiothreitol (DTT)]. Cells were lysed with a sonic dismembrator at 4 °C. GST-SNAP25 was purified from cleared lysates by affinity chromatography on glutathione-agarose (GE Healthcare), following the manufacturer's instructions. While the proteins were bound to the column, the buffer was exchanged to 20 mM HEPES, pH 7.4, 100 mM NaCl, 0.05% *n*-octyl β-D-glucopyranoside (OG), and 5 mM DTT. The proteins were eluted by cleaving from GST with PreScission protease (GE Healthcare) for 4 h at 4 °C. GST-H3 domain of syntaxin1A was purified from the sonicated bacterial supernatant by affinity chromatography on glutathione-agarose (GE Healthcare) in 10 mM HEPES, pH 7.4, 0.05% OG, and 2 mM DTT. Protein concentrations were determined with a Bradford assay kit (Pierce, Rockford, IL), and purity was verified by SDS/PAGE analysis.

t-SNARE Complex Reassembly. A slight excess of SNAP25 (4 μM) to GST-H3 (3 μM) on glutathione-agarose beads was incubated overnight at 4 °C in 20 mM HEPES, pH 7.4, 100 mM NaCl, 0.1% OG, and 2.0 mM DTT. The binary t-SNARE complex (SNAP25 with the H3 domain of syntaxin 1A) was washed three times with phosphate-buffered saline and eluted from the column by removing GST with PreScission protease (GE Healthcare) for 4 h at 4 °C. Equimolar protein−protein interaction was confirmed by SDS-PAGE/Coomassie staining analysis.

$G\beta\gamma$ Purification. $G\beta_1\gamma_1$ was purified from bovine retina as described previously.[34] Recombinant $G\beta_1\gamma_2$ was expressed in Sf9 cells and purified via a His6 tag on $G\gamma_2$ using nickel-nitrilotriacetic acid affinity chromatography (Sigma-Aldrich, St. Louis, MO).

Resonant Waveguide Grating Biosensor Detection. A beta version of the Corning EPIC was used for all experiments. The details of this system have been previously described.[35,36] Briefly, binding interactions between $G\beta\gamma$ subunits and SNARE proteins were evaluated using a novel, label-free system from Corning, called the EPIC, which allows detection of protein−protein interactions without the need for fluorescent- or radio-labeling. The system comprises two components: an optical reader and a 384 well microplate containing an

dx.doi.org/10.1021/cn200102d | *ACS Chem. Neurosci.* 2012, 3, 69–78

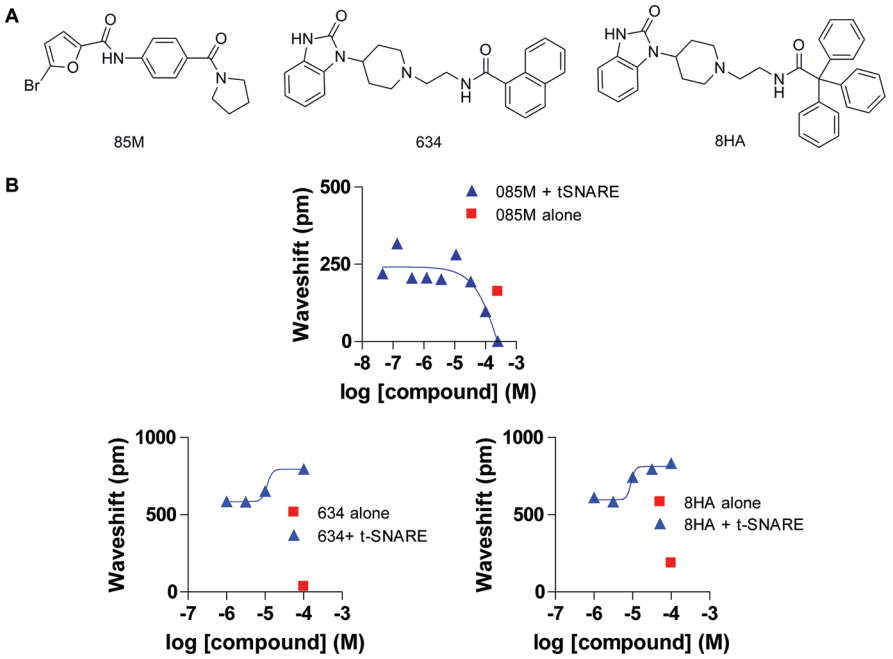

Figure 7. Concentration response curves for compounds that inhibit or enhance binding between G$\beta\gamma$ and t-SNARE. (A) Shown are the chemical compounds (85M, 634, and 8HA) that had significantly affected the waveshift of the interaction between t-SNARE and immobilized G$\beta_1\gamma_1$. (B) Compounds 85M, 634, and 8HA were tested in a concentration dependent manner on the detected waveshift of constant t-SNARE concentration exposed to immobilized G$\beta_1\gamma_1$. Shown are the concentration response curves from those compounds. Each point in the three concentration response curves represents the average of four wells on a plate.

optical sensor within each well, known as a RWG. When plates are illuminated with broadband light, one dominant wavelength of light resonates within the waveguide, and is strongly reflected. The addition of proteins to the surface of the plate, however, changes the local index of refraction, changing the resonant wavelength that is reflected (known as a waveshift). These waveshifts (measured in picometers (pm)) can therefore be used to evaluate protein−protein interactions. Further, each well is partitioned to allow for self-referencing. This is accomplished by only applying binding chemistry to one-half of each well, thereby allowing for simultaneous measurement of target protein interactions with immobilized partners as well as interactions with the well surface itself.

Detection of t-SNARE (SNAP25-syntaxin1A H3) on the EPIC. The initial step of the assay is the immobilization of either G$\beta_1\gamma_1$ or G$\beta_1\gamma_2$ to the plate. A variety of conditions were explored as described in the Results and Discussion section. The resulting common immobilization protocol from this work was the addition of 25 μg/mL of either G$\beta_1\gamma_1$ or G$\beta_1\gamma_2$ in 20 mM sodium acetate, pH 5.0 and 5% glycerol to the respective wells overnight at 4 °C. This time frame ensured quenching the plate chemistry that did not react with G$\beta\gamma$. The following day, wells were then washed twice with 20 mM sodium acetate, pH 5.0, with 5% glycerol followed by two washes with a common HEPES binding buffer (20 mM HEPES, pH 7.5, 5% glycerol, 2 mM magnesium chloride, 10 uM guanosine diphosphate (GDP), and 5% DMSO). This HEPES binding buffer was determined by a series of experiments to determine the tolerances of the microplate and of the detection of interaction between immobilized G$\beta\gamma$ and t-SNARE. The plates were allowed to thermally equilibrate in the EPIC before an initial immobilization read was done. Purified t-SNARE or other binding partners were then added to wells, and the plate was allowed to re-equilibrate for 1 h before a binding reading was done. Figure error bars represent within-experiment errors based on each plate tested.

Chemical Synthesis and Purification. All ^{1}H and ^{13}C NMR spectra were recorded on Bruker AV-400 (400 MHz) or Bruker AV-NMR (600 MHz) instrument. Chemical shifts are reported in ppm relative to residual solvent peaks as an internal standard set to δH 7.26 or δC 77.0 ($CDCl_3$) and δH 3.31 or δC 49.0 (CD_3OD). Data are reported as follows: chemical shift, multiplicity (s = singlet, d = doublet, t = triplet, q = quartet, br = broad, m = multiplet), integration, coupling constant (Hz). IR spectra were recorded as thin films and are reported in wavenumbers (cm^{-1}). Low resolution mass spectra were obtained on an Agilent 1200 LCMS with electrospray ionization. High resolution mass spectra were recorded on a Waters Qtof-API-US plus Acquity system. The value Δ is the error in the measurement (in ppm) given by the equation $\Delta = [(M_E - M_T)/ M_T] \times 106$, where M_E is the experimental mass and M_T is the theoretical mass. The HRMS results were obtained with ES as the ion source and leucine enkephalin as the reference. Optical rotations were measured on a Perkin-Elmer-341 polarimeter. Analytical thin layer chromatography was performed on 250 μM silica gel 60 F254 plates. Visualization was accomplished with UV light, and/or the use of ninhydrin, anisaldehyde and ceric ammonium molybdate solutions followed by charring on a hot-plate. Chromatography on silica gel was performed using Silica Gel 60 (230−400 mesh) from Sorbent Technologies. Analytical HPLC was performed on an Agilent 1200 analytical LCMS with UV detection at 214 and 254 nm along with ELSD detection. Solvents for extraction, washing and chromatography were HPLC grade. All reagents were purchased from Aldrich Chemical Co. and were used without purification. All polymer-supported reagents were purchased from Biotage, Inc. Flame-dried (under vacuum) glassware was used for all reactions. All reagents and solvents were commercial grade and purified prior to use when necessary. Mass spectra were obtained on a Micromass Q-Tof API-US mass spectrometer was used to acquire high-resolution mass spectrometry (HRMS) data.

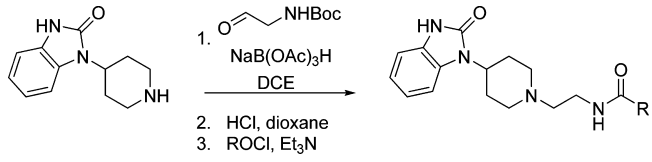

General Procedure. To a 10 mL vial was placed 1-(piperidin-4-yl)-1*H*-benzo[*d*]imidazol-2(3*H*)-one (0.1 mmol) and diluted with 2 mL of DCE, followed by *tert*-butyl 2-oxoethylcarbamate (0.12 mmol). $NaB(OAc)_3H$ (0.25 mmol) was added and the vial placed on a rotator

dx.doi.org/10.1021/cn200102d | *ACS Chem. Neurosci.* 2012, 3, 69−78

for 6 h, followed by an aqueous wash and extraction with DCM (2 × 5 mL). The crude extract was then treated with 4.0 M HCL in dioxane for 1 h, which provided full deprotection of the Boc group, and uniformly affording the crude primary amine in >95% purity as judged by LCMS and NMR. Finally, the crude amine was dissolved in DCM, Et_3N added (1.5 equiv), and one of 48 ROCls (1.2 equiv) added and allowed to rotate for 24 h. Concentration and mass-directed HPLC afforded the final compounds in excellent yields (70−99%) and purity (>98%).

Screening of the Ligand Library. Microtiter plates with immobilized G$\beta\gamma$ were prepared as above. Compounds were then added at a concentration of 250 μM individually to groups of at least four wells in the presence of t-SNARE. To assess nonspecific waveshift changes induced by interaction of the compounds with either G$\beta\gamma$ or the plate itself, at least four wells were exposed to compound alone. The difference between the waveshift of compound alone with G$\beta\gamma$ and in the presence of t-SNARE was defined as the effect of the compound on the interaction between G$\beta\gamma$ and t-SNARE. For select "hits" that produced a significant change from waveshifts seen for t-SNARE binding to G$\beta\gamma$ alone, a concentration response curve was determined with at least four wells for each concentration of compound.

AUTHOR INFORMATION

Corresponding Author

*E-mail: heidi.hamm@Vanderbilt.edu. Telephone: 615-343-3533. Fax: 615-343-1084.

Author Contributions

†These authors contributed equally to this work.

Author Contributions

C.A.W. and K.M.B. performed the methods, experimental work, data analysis, manuscript writing, and preparation equally. K.M.B. and C.W.L. developed the chemical library and the iterative compounds. H.E.H. and C.W.L. provided guidance and advice as well as assistance with manuscript writing and preparation.

Funding

Research in the authors' laboratory was supported by a grant from the National Institute of Health, R01 EY010291. CAW was supported by the T32 Training in Cardiovascular Research Grant T32 HL007411. C.W.L. was supported by funding from the Department of Pharmacology, Vanderbilt University.

Notes

The authors declare no competing financial interest.

In the interim, between performing the experiments and publication of this article, the technology for this assay was licensed by Corning to Perkin-Elmer. All of these experiments included in this manuscript were performed on the Corning EPIC device. However, similar experiments were repeated on this new system from Perkin-Elmer (EnSpire) with no change in the quality, reproducibility, or significance of the results (data not shown).

ACKNOWLEDGMENTS

We would like to thank Ravi Marala and Alice Gao from Corning for their technical assistance in developing this assay with their EPIC system.

ABBREVIATIONS

BSA, bovine serum albumin; HEPES, 4-(2-hydroxyethyl)-1-piperazineethanesulfonic acid; CHAPS, 3-[(3-cholamidopropyl)dimethylammonio]-1-propanesulfonate; DTT, dithiothreitol; SNARE, soluble *N*-ethylmaleimide-sensitive factor attachment protein receptors; GDP, guanosine diphosphate; $GTP_\gamma S$, guanosine 5′-*O*-[gamma-thio]-triphosphate; RWG, resonant waveguide

REFERENCES

(1) Gerachshenko, T., Blackmer, T., Yoon, E. J., Bartleson, C., Hamm, H. E., and Alford, S. (2005) G$\beta\gamma$ acts at the C terminus of SNAP-25 to mediate presynaptic inhibition. *Nat. Neurosci. 8*, 597−605.

(2) Yoon, E. J., Gerachshenko, T., Spiegelberg, B. D., Alford, S., and Hamm, H. E. (2007) Gbetagamma interferes with Ca2+-dependent binding of synaptotagmin to the soluble N-ethylmaleimide-sensitive factor attachment protein receptor (SNARE) complex. *Mol. Pharmacol. 72*, 1210−1219.

(3) Blackmer, T., Larsen, E. C., Bartleson, C., Kowalchyk, J. A., Yoon, E. J., Preininger, A. M., Alford, S., Hamm, H. E., and Martin, T. F. (2005) G protein betagamma directly regulates SNARE protein fusion machinery for secretory granule exocytosis. *Nat. Neurosci. 8*, 421−425.

(4) Parpura, V., and Mohideen, U. (2008) Molecular form follows function: (un)snaring the SNAREs. *Trends Neurosci. 31*, 435−443.

(5) Jahn, R., and Scheller, R. H. (2006) SNAREs--engines for membrane fusion. *Nat. Rev. Mol. Cell Biol. 7*, 631−643.

(6) Geppert, M., Goda, Y., Hammer, R. E., Li, C., Rosahl, T. W., Stevens, C. F., and Sudhof, T. C. (1994) Synaptotagmin I: a major Ca2+ sensor for transmitter release at a central synapse. *Cell 79*, 717−727.

(7) Sudhof, T. C. (2004) The synaptic vesicle cycle. *Annu. Rev. Neurosci. 27*, 509−547.

(8) Currie, K. P. (2010) Inhibition of Ca2+ channels and adrenal catecholamine release by G protein coupled receptors. *Cell. Mol. Neurobiol. 30*, 1201−1208.

(9) Herlitze, S., Garcia, D. E., Mackie, K., Hille, B., Scheuer, T., and Catterall, W. A. (1996) Modulation of Ca2+ channels by G-protein beta gamma subunits. *Nature 380*, 258−262.

(10) Ikeda, S. R. (1996) Voltage-dependent modulation of N-type calcium channels by G-protein beta gamma subunits. *Nature 380*, 255−258.

(11) Tedford, H. W., Kisilevsky, A. E., Peloquin, J. B., and Zamponi, G. W. (2006) Scanning Mutagenesis Reveals a Role for Serine 189 of the Heterotrimeric G-Protein Beta 1 Subunit in the Inhibition of N-Type Calcium Channels. *J. Neurophysiol. 96*, 465−470.

(12) Tedford, H. W., and Zamponi, G. W. (2006) Direct G Protein Modulation of Cav2 Calcium Channels. *Pharmacol. Rev. 58*, 837−862.

(13) Straiker, A. J., Borden, C. R., and Sullivan, J. M. (2002) G-Protein α Subunit Isoforms Couple Differentially to Receptors that Mediate Presynaptic Inhibition at Rat Hippocampal Synapses. *J. Neurosci. 22*, 2460−2468.

(14) Blackmer, T., Larsen, E. C., Takahashi, M., Martin, T. F., Alford, S., and Hamm, H. E. (2001) G protein betagamma subunit-mediated presynaptic inhibition: regulation of exocytotic fusion downstream of Ca2+ entry. *Science 292*, 293−297.

(15) Gerachshenko, T., Blackmer, T., Yoon, E. J., Bartleson, C., Hamm, H. E., and Alford, S. (2005) Gbetagamma acts at the C terminus of SNAP-25 to mediate presynaptic inhibition. *Nat. Neurosci. 8*, 597−605.

(16) Zhao, Y., Fang, Q., Straub, S. G., Lindau, M., and Sharp, G. W. (2010) Noradrenaline inhibits exocytosis via the G protein betagamma subunit and refilling of the readily releasable granule pool via the alpha(i1/2) subunit. *J. Physiol. 588*, 3485−3498.

(17) Yoon, E. J., Hamm, H. E., and Currie, K. P. M. (2008) G protein beta gamma subunits modulate the number and nature of exocytotic fusion events in adrenal chromaffin cells independent of calcium entry. *J. Neurophysiol. 100*, 2929−2939.

(18) Delaney, A. J., Crane, J. W., and Sah, P. (2007) Noradrenaline Modulates Transmission at a Central Synapse by a Presynaptic Mechanism. *Neuron 56*, 880−892.

(19) Zhang, X.-l., Upreti, C., and Stanton, P. K. (2011) G$\beta\gamma$ and the C Terminus of SNAP-25 Are Necessary for Long-Term Depression of Transmitter Release. *PLoS One 6*, e20500.

(20) Cooper, M. (2003) Label-free screening of bio-molecular interactions. *Anal. Bioanal. Chem. 377*, 834−842.

(21) Shiau, A. K., Massari, M. E., and Ozbal, C. C. (2008) Back to basics: label-free technologies for small molecule screening. *Combinatorial Chem. High Throughput Screening 11*, 231−237.
(22) Cooper, M. A. (2006) Optical biosensors: where next and how soon? *Drug Discovery Today 11*, 1061−1067.
(23) Fang, Y. (2011) Label-Free Biosensors for Cell Biology. *Int. J. Electrochem.*, DOI: 10.4061/2011/460850.
(24) Lavieri, R., Scott, S. A., Lewis, J. A., Selvy, P. E., Armstrong, M. D., Alex Brown, H., and Lindsley, C. W. (2009) Design and synthesis of isoform-selective phospholipase D (PLD) inhibitors. Part II. Identification of the 1,3,8-triazaspiro[4,5]decan-4-one privileged structure that engenders PLD2 selectivity. *Bioorg. Med. Chem. Lett. 19*, 2240−2243.
(25) Lavieri, R. R., Scott, S. A., Selvy, P. E., Kim, K., Jadhav, S., Morrison, R. D., Daniels, J. S., Brown, H. A., and Lindsley, C. W. (2010) Design, synthesis, and biological evaluation of halogenated N-(2-(4-oxo-1-phenyl-1,3,8-triazaspiro[4.5]decan-8-yl)ethyl)benzamides: discovery of an isoform-selective small molecule phospholipase D2 inhibitor. *J. Med. Chem. 53*, 6706−6719.
(26) Lewis, J. A., Scott, S. A., Lavieri, R., Buck, J. R., Selvy, P. E., Stoops, S. L., Armstrong, M. D., Brown, H. A., and Lindsley, C. W. (2009) Design and synthesis of isoform-selective phospholipase D (PLD) inhibitors. Part I: Impact of alternative halogenated privileged structures for PLD1 specificity. *Bioorg. Med. Chem. Lett. 19*, 1916−1920.
(27) Lindsley, C. W., Zhao, Z., Leister, W. H., Robinson, R. G., Barnett, S. F., Defeo-Jones, D., Jones, R. E., Hartman, G. D., Huff, J. R., Huber, H. E., and Duggan, M. E. (2005) Allosteric Akt (PKB) inhibitors: discovery and SAR of isozyme selective inhibitors. *Bioorg. Med. Chem. Lett. 15*, 761−764.
(28) Scott, S. A., Selvy, P. E., Buck, J. R., Cho, H. P., Criswell, T. L., Thomas, A. L., Armstrong, M. D., Arteaga, C. L., Lindsley, C. W., and Brown, H. A. (2009) Design of isoform-selective phospholipase D inhibitors that modulate cancer cell invasiveness. *Nat. Chem. Biol. 5*, 108−117.
(29) Zhao, Z., Leister, W. H., Robinson, R. G., Barnett, S. F., Defeo-Jones, D., Jones, R. E., Hartman, G. D., Huff, J. R., Huber, H. E., Duggan, M. E., and Lindsley, C. W. (2005) Discovery of 2,3,5-trisubstituted pyridine derivatives as potent Akt1 and Akt2 dual inhibitors. *Bioorg. Med. Chem. Lett. 15*, 905−909.
(30) Arkin, M. R., and Wells, J. A. (2004) Small-molecule inhibitors of protein-protein interactions: progressing towards the dream. *Nat. Rev. Drug Discovery 3*, 301−317.
(31) Blazer, L. L., and Neubig, R. R. (2009) Small molecule protein-protein interaction inhibitors as CNS therapeutic agents: current progress and future hurdles. *Neuropsychopharmacology 34*, 126−141.
(32) Gerachshenko, T., Schwartz, E., Bleckert, A., Photowala, H., Seymour, A., and Alford, S. (2009) Presynaptic G-protein-coupled receptors dynamically modify vesicle fusion, synaptic cleft glutamate concentrations, and motor behavior. *J. Neurosci. 29*, 10221−10233.
(33) Yoon, E. J., Hamm, H. E., and Currie, K. P. (2008) G protein betagamma subunits modulate the number and nature of exocytotic fusion events in adrenal chromaffin cells independent of calcium entry. *J. Neurophysiol. 100*, 2929−2939.
(34) Mazzoni, M. R., Malinski, J. A., and Hamm, H. E. (1991) Structural analysis of rod GTP-binding protein, Gt. Limited proteolytic digestion pattern of Gt with four proteases defines monoclonal antibody epitope. *J. Biol. Chem. 266*, 14072−14081.
(35) Fang, Y., Ferrie, A. M., Fontaine, N. H., Mauro, J., and Balakrishnan, J. (2006) Resonant Waveguide Grating Biosensor for Living Cell Sensing. *Biophys. J. 91*, 1925−1940.
(36) Fang, Y., Ferrie, A. M., Fontaine, N. H., and Yuen, P. K. (2005) Characteristics of dynamic mass redistribution of epidermal growth factor receptor signaling in living cells measured with label-free optical biosensors. *Anal. Chem. 77*, 5720−5725.